

## Upper critical field and normal-state properties of single-phase $Y_{1-x}Pr_xBa_2Cu_3O_{7-\delta}$ compounds

J. L. Peng, P. Klavins, and R. N. Shelton

*Department of Physics, University of California, Davis, Davis, California 95616*

H. B. Radousky, P. A. Hahn, and L. Bernardez

*Lawrence Livermore National Laboratory, P.O. Box 808, Livermore, California 94550*

(Received 10 April 1989)

Substitution of Pr for Y in the  $Y_{1-x}Pr_xBa_2Cu_3O_{7-\delta}$  system depresses  $T_c$ , with superconductivity disappearing for  $x \geq 0.5$ . The origin of this  $T_c$  depression is still controversial, as is the valence state of the Pr ion. In order to study these problems, single-phase materials were prepared with  $x = 0.0, 0.1, 0.2, 0.3, 0.35, 0.4, 0.45, 0.5, 0.6, 0.7, 0.9,$  and  $1.0$ . Under certain annealing conditions, these types of samples will phase separate into  $YBa_2Cu_3O_{7-\delta}$  and  $Y_{1-x}Pr_xBa_2Cu_3O_{7-\delta}$ , showing two transitions in the magnetization, and will still appear single phase from x-ray diffraction. We have overcome this problem through specific annealing conditions of time, temperature, and atmosphere. We find that the superconductivity is strongly suppressed as a function of Pr concentration, with a behavior which is consistent with the classical Abrikosov-Gor'kov pair-breaking theory. The critical fields versus  $T$  show a "bell"-shaped behavior, which is consistent with the presence of magnetic pair-breaking interactions. The measured temperature dependence of the critical field,  $H_{c2}$  near  $T_c$ , and the Pauli susceptibility, are used to estimate the physical parameters  $\lambda_{GL}$ ,  $\xi_{GL}$ , and  $\gamma$ .

### INTRODUCTION

The discovery of superconductivity with transition temperatures ( $T_c$ ) in the 90-K range in  $YBa_2Cu_3O_{7-\delta}$  (Ref. 1) has generated a great deal of interest in the oxide superconductors. The substitution of Y by trivalent rare-earth elements, with the exception of Ce, Pr, Pm, and Tb, yields a superconducting phase with a  $T_c$  almost identical to the  $YBa_2Cu_3O_{7-\delta}$  compound.<sup>2-5</sup> Samples of  $RBa_2Cu_3O_{7-\delta}$  with  $R = Ce$  and  $Tb$  prepared by the standard solid-state reaction technique<sup>6</sup> yield multiphase materials consisting of  $BaCeO_3$  or  $BaTbO_3$ ,  $CuO$ , and  $BaCuO_2$ , which are not superconducting. No investigations have been reported for the  $PmBa_2Cu_3O_{7-\delta}$  compound because the Pm nucleus is radioactively unstable. The  $Y_{1-x}Pr_xBa_2Cu_3O_{7-\delta}$  system is particularly interesting since it is isostructural to the  $YBa_2Cu_3O_{7-\delta}$  superconductor, yet the superconductivity is strongly suppressed as a function of Pr concentration.<sup>7-9</sup> This quenching of the superconducting state is not understood in detail. Extensive measurements have been carried out as a function of Pr concentration which include magnetization,<sup>10-13</sup> heat-capacity,<sup>14</sup> thermopower,<sup>15</sup> Hall effect,<sup>11</sup> neutron-diffraction,<sup>16</sup> pressure effects,<sup>17</sup> x-ray-absorption,<sup>18,19</sup> and Raman spectroscopy.<sup>20,21</sup> The effect of the Pr ion on the superconducting properties may help our understanding of the interplay between magnetism and superconductivity and provide insight as to the origin of the superconductivity in the high- $T_c$  oxides.

One problem in studying the  $Y_{1-x}Pr_xBa_2Cu_3O_{7-\delta}$  system is its tendency to phase separate into  $YBa_2Cu_3O_{7-\delta}$  with  $T_c = 90$  K and  $Y_{1-x}Pr_xBa_2Cu_3O_{7-\delta}$  of varying  $x$  value and a reduced  $T_c$ . This type of phase separation

can be clearly seen in the field-cooled Meissner measurements,<sup>22</sup> while not showing up at all in the powder x-ray-diffraction patterns. The resistivity data on these phase-separated samples showed broad transitions. We have overcome this problem through specific annealing conditions of time, temperature, and atmosphere. All samples reported in this paper were observed to have less than 1% phase separation from field-cooled magnetization.

We report the preparation, structure, oxygen content, resistivity, magnetization, and critical field in the single-phase  $Y_{1-x}Pr_xBa_2Cu_3O_{7-\delta}$  system. The electronic coefficient of specific heat,  $\gamma$ , the density of states,  $N(0)$ , and the Ginzburg-Landau parameters,  $\xi_{GL}$ ,  $\lambda_{GL}$ , and  $\kappa_{GL}$ , are estimated along with the exchange interaction parameter  $\mathcal{J}$ , from the measured temperature dependence of  $H_{c2}$  and the Pauli susceptibility.

### EXPERIMENTAL DETAILS

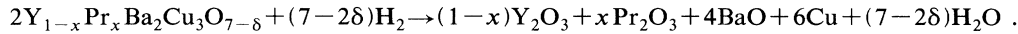
Samples of  $Y_{1-x}Pr_xBa_2Cu_3O_{7-\delta}$  were prepared for  $x = 0.0, 0.1, 0.2, 0.3, 0.35, 0.4, 0.45, 0.5, 0.6, 0.7, 0.9,$  and  $1.0$ . Starting from high-purity  $Y_2O_3$ ,  $BaO$ ,  $CuO$ , and  $Pr_6O_{11}$ , the powders were mixed and fired in air at  $975^\circ C$  for about 50 h. The powders were cooled to room temperature by air quenching. Next, the powders were re-ground and fired at  $1000-1010^\circ C$  for 48 h with several intermediate regrindings. The loose powder was then pressed into a pellet and annealed in flowing oxygen for two hours at  $975^\circ C$ , before furnace cooling to  $400^\circ C$ . The pellet was finally annealed in flowing oxygen at  $400^\circ C$  for 24 h followed by furnace cooling to room temperature.

Powder x-ray-diffraction data were taken for all samples of  $Y_{1-x}Pr_xBa_2Cu_3O_{7-\delta}$  using Cu  $K\alpha$  radiation at room temperature. The lattice parameters were calculated from the diffraction peak positions by the method of least squares. The x-ray-diffraction patterns indicated that the single-phase orthorhombic structure persists throughout the composition range  $0 \leq x < 0.9$ , while for  $x \geq 0.9$ , a single-phase tetragonal structure was observed. The key feature that demonstrated the orthorhombic-to-tetragonal transition is the convergence of the (012, 102), (013, 103), (020, 200), (122, 212), and (123, 213) reflections. Within the instrumental resolution, no im-

purity phases were observed.

The oxygen content of all materials was determined by thermogravimetric analysis (TGA), using a Dupont 951 TGA system. The typical starting sample mass was approximately 50 mg, with a balance resolution of 2  $\mu$ g. A single scan involved flowing forming gas (6 at. %  $H_2$ , 94 at. %  $N_2$ ) through the sample chamber and ramping the temperature from 30 °C to 1000 °C at a rate of 5 °C/min. Oxygen loss was observed as early as 400 °C with mass loss saturating by 900 °C.

The reduction reaction has been empirically established as



By monitoring the weight change of  $Y_{1-x}Pr_xBa_2Cu_3O_{7-\delta}$  in the reducing atmosphere, the absolute value of  $\delta$  can be obtained. A small amount of Ba-CuO<sub>2</sub> (~1%) was observed in some of the samples from Raman analysis.<sup>21</sup> This was not included in the TGA calculation and introduced an error of  $\approx 0.02$  in the oxygen contents for those samples. The total error is conservatively estimated to be  $\pm 0.04$ .

Electrical resistivity  $\rho(T)$  measurements were performed on rectangular specimens cut from sintered pellets employing the standard dc four-probe technique with silver paint contacts attached electrical leads. Data were collected from 300 down to 10 K.

The dc magnetic susceptibility for each sample was measured with a superconducting quantum interference device (SQUID) magnetometer (Quantum Design) over the temperature range 2–350 K. A field of 10 Oe was used to measure the Meissner effect and a field of 5 kOe was used to measure the susceptibility above  $T_c$ , from which the temperature-independent susceptibility ( $\chi_0$ ), Curie-Weiss temperature ( $\Theta$ ), and the effective magnetic moment ( $\mu_{\text{eff}}$ ) could be derived. The upper critical field  $H_{c2}$  up to 50 kOe was measured magnetically with the SQUID magnetometer.

## RESULTS

The lattice parameters  $a$ ,  $b$ ,  $c$  and the cell volume  $V$  for the single-phase  $Y_{1-x}Pr_xBa_2Cu_3O_{7-\delta}$  obtained from x-ray diffraction are plotted in Fig. 1 as a function of the Pr composition. While the lattice parameters  $a$  and  $b$  both increase with Pr composition, the  $a$  parameter depends more dramatically on the Pr concentration. The lattice parameter  $c$  remains essentially unchanged with doping. The unit-cell volume increases rapidly with increasing  $x$ . The orthorhombic distortion is reduced by the substitution of Pr. A transition in crystal symmetry from orthorhombic to tetragonal occurs in these samples at about  $x = 0.9$ .

The oxygen stoichiometries determined by TGA are given in Table I along with the lattice parameters. The nonsuperconducting samples ( $x \geq 0.5$ ) show an oxygen content of  $7.00 \pm 0.04$ , while the oxygen content of super-

conducting samples ( $x < 0.5$ ) varies from 6.88 to 7.01. Such a change in oxygen content ( $-0.03 < \delta < 0.12$ ) is due to the variation of the experimental condition for each sample preparation. In fact, it is possible to prepare

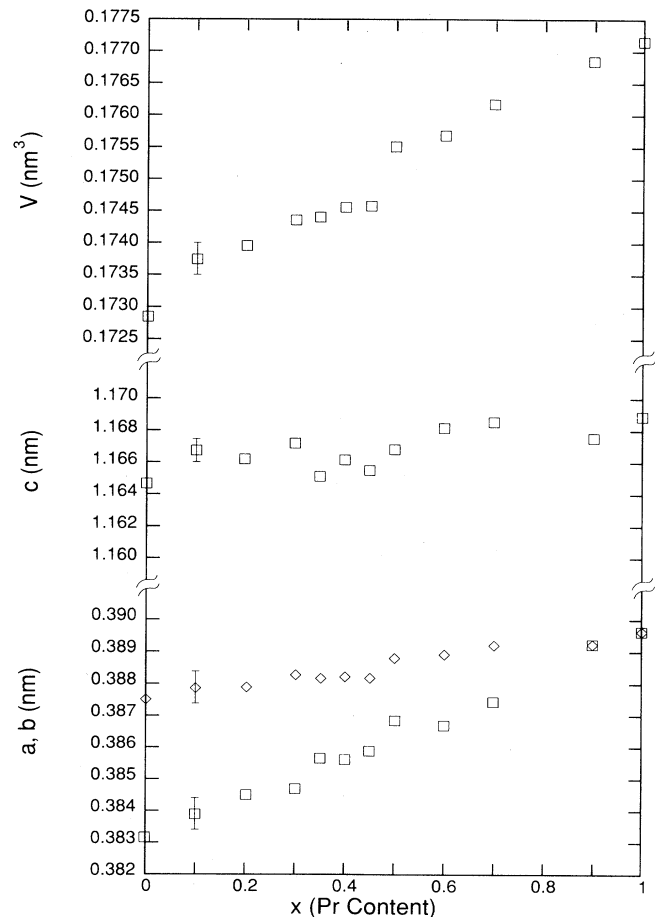


FIG. 1. Lattice parameters  $a$  (□),  $b$  (◇),  $c$ , and unit-cell volume  $V$  determined by powder x-ray diffraction as a function of Pr content at room temperature.

TABLE I. Oxygen content and lattice parameters of  $Y_{1-x}Pr_xBa_2Cu_3O_{7-\delta}$ .

$x$	Oxygen content	$a$ (nm)	$b$ (nm)	$c$ (nm)	$V$ (nm <sup>3</sup> )
0.0	6.96	0.3831	0.3875	1.1646	0.1729
0.1	6.91	0.3839	0.3879	1.1668	0.1738
0.2	6.91	0.3845	0.3879	1.1662	0.1739
0.3	6.88	0.3847	0.3883	1.1672	0.1744
0.35	7.01	0.3857	0.3882	1.1652	0.1744
0.4	6.90	0.3856	0.3882	1.1662	0.1746
0.45	7.01	0.3859	0.3882	1.1655	0.1746
0.5	7.01	0.3868	0.3888	1.1669	0.1755
0.6	7.03	0.3867	0.3889	1.1682	0.1757
0.7	7.03	0.3874	0.3892	1.1686	0.1762
0.9	7.03	0.3892	0.3892	1.1675	0.1769
1.0	6.96	0.3896	0.3896	1.1688	0.1771

all samples with an oxygen content of  $7.0 \pm 0.04$ . Doping with Pr on the Y sites in the  $YBa_2Cu_2O_7$  structure does not significantly affect oxygen concentration. This is not unexpected, as the Pr ions are situated between stable Cu—O planes with full oxygen occupancy rather than adjacent to the oxygen deficient Cu—O chain layers in which oxygen is considerably more mobile. Recent neutron-diffraction studies<sup>17</sup> indicate that the oxygen content remains essentially constant for  $x = 0.2, 0.4, 0.6,$  and  $1.0$ . This is consistent with our results. In addition, the differential thermal analysis (DTA) confirmed the phase purity for these Pr-doped compounds in our studies.

In Fig. 2 we present  $4\pi M$  versus  $T$  for samples of  $x = 0, 0.1, 0.2, 0.3, 0.35,$  and  $0.45$  cooled in the field of 10 Oe.

The superconducting transition temperature ( $T_c$ ) decreases monotonically, with samples for  $x \geq 0.5$  showing no superconductivity above 2.0 K. All samples showed only one superconducting transition, with transition widths remaining rather narrow.

Electrical resistivity  $\rho(T)$  data for the series of  $Y_{1-x}Pr_xBa_2Cu_3O_{7-\delta}$  ( $0 \leq x \leq 1$ ) are shown in Fig. 3. As  $x$  increases, the temperature coefficient of resistivity of the normal state decreases continuously and changes from positive to negative at  $x = 0.35$  as the resistive superconductive transition curves shift to lower temperatures. For low dopant concentrations ( $x < 0.3$ ), the resistivity shows a metallic-like behavior; however, the resistivity curves at  $x = 0.3, 0.35, 0.4,$  and  $0.45$  display a broad maximum just above  $T_c$ . The value of the resistivi-

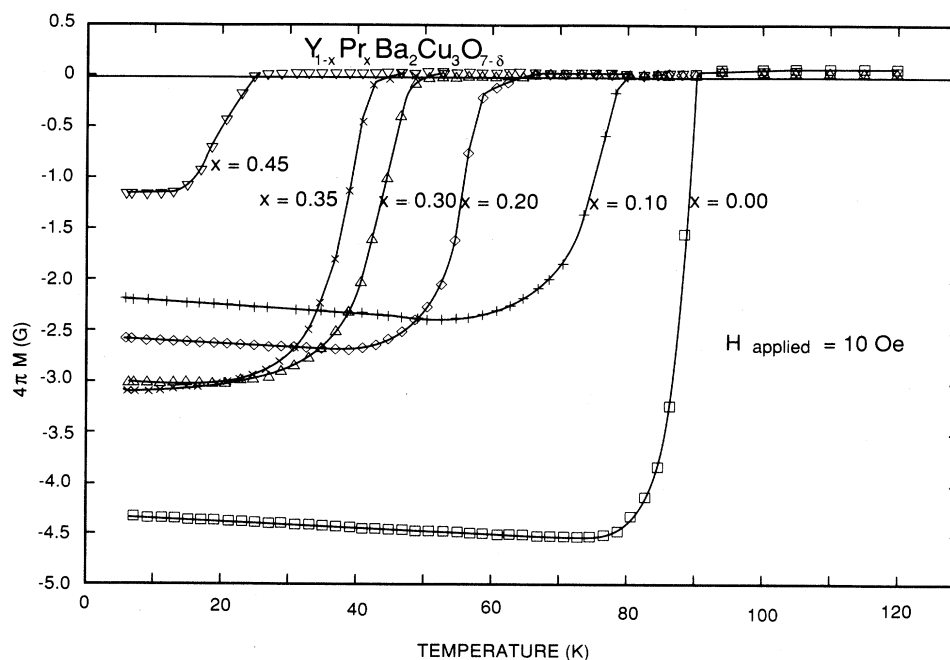


FIG. 2. Field-cooled magnetization ( $4\pi M$ ) vs temperature as measured with a SQUID magnetometer in a field of 10 Oe.

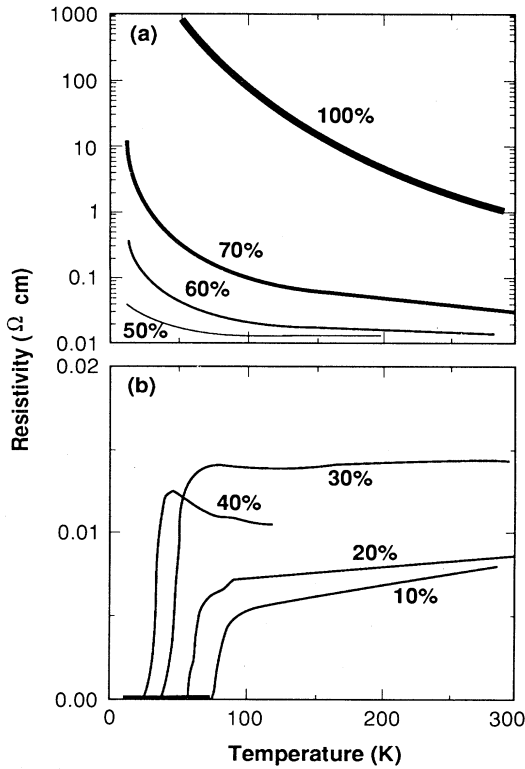


FIG. 3. Electrical resistivity  $\rho(T)$  for the series of  $Y_{1-x}Pr_xBa_2Cu_3O_{7-\delta}$  ( $0 \leq x \leq 1$ ) as a function of temperature.

ty at 100 K increases dramatically for  $x \geq 0.7$  as shown in Fig. 4. These experimentally determined values of the resistivity are considerably higher than values deduced from the theoretical analysis based on the Ginzberg-Landau approach and presented later on in connection with the critical-field data. This discrepancy may be due

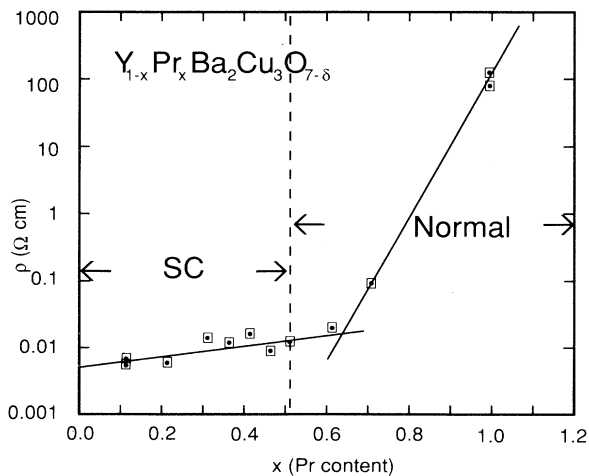


FIG. 4. Electrical resistivity at 100 K as a function of Pr content. Superconducting (SC) and normal regions are indicated.

to grain boundary resistance, effect of anisotropy, and sample densities of pressed powder compacts that are well below the theoretical density.

In general, superconductivity is affected strongly by the presence of magnetic impurities which interact directly with the superconducting electrons through the conduction-electron-impurity-spin exchange interaction and break the Cooper pairs, thereby suppressing  $T_c$ . The absence of a correlation between the superconducting properties of the  $RBa_2Cu_3O_{7-\delta}$  ( $R$  = rare-earth element, except Ce, Pr, and Tb) compounds and the magnetism of the rare-earth element, suggests that the superconducting electrons in these types of materials do not interact with the magnetic ions. However, the presence of Pr ions in  $YBa_2Cu_3O_{7-\delta}$  rapidly depresses the  $T_c$ .<sup>7-9</sup> The transition temperatures ( $T_c$ ) determined by the midpoints of the resistive data are plotted in Fig. 5 with the 10–90% widths ( $\Delta T_c$ ) indicated by vertical bars. We note that the superconductivity disappears for  $x \geq 0.05$ , while the  $Y_{1-x}Pr_xBa_2Cu_3O_{7-\delta}$  compounds possess an orthorhombic structure for  $x < 0.9$ .

The normal-state magnetic susceptibility data up to 300 K can be expressed as

$$\chi(T) = \chi_0 + C / (T - \Theta), \quad (1)$$

where  $\chi_0$  is a temperature-independent component of the susceptibility and  $C / (T - \Theta)$  is the Curie-Weiss contribution. Values of  $\chi_0$ ,  $C$ , and  $\Theta$  were obtained by a non-linear least-squares fit. The temperature-independent susceptibility  $\chi_0$  versus Pr content  $x$  is plotted in Fig. 6.  $\chi_0$  increases with increasing  $x$ . The Curie-Weiss coefficient  $C$  (proportional to the number of local moments) increases proportional to the Pr concentration, while the Curie-Weiss temperature is only weakly concentration dependent. In order to calculate the effective moment of the Pr ion from the  $\chi(T)$  data of the series of  $Y_{1-x}Pr_xBa_2Cu_3O_{7-\delta}$ , the contribution to  $\chi(T)$  of the

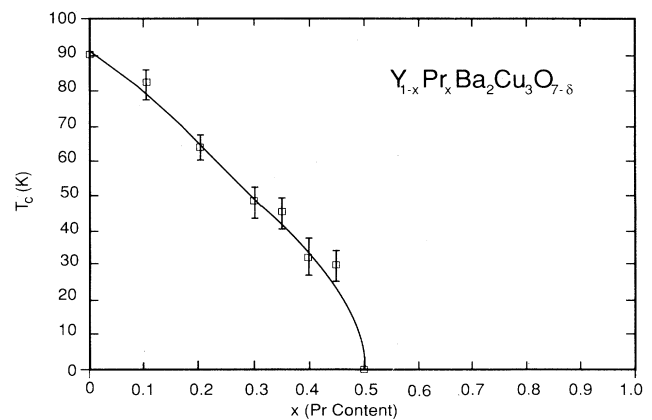


FIG. 5. The transition temperature ( $T_c$ ) determined by the midpoints of the resistivity data as a function of Pr content. The vertical bars indicate the 10–90% resistivity transition widths ( $\Delta T_c$ ). The solid line is a fit of  $T_c$  vs  $x$  by the Abrikosov and Gor'kov theory.

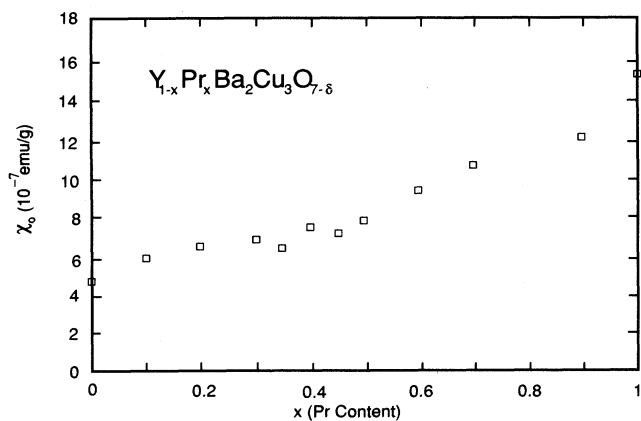


FIG. 6. The temperature-independent susceptibility  $\chi_0$  vs Pr content  $x$ , obtained by the nonlinear least-squares fit of the magnetic-susceptibility data.

host compound  $\text{YBa}_2\text{Cu}_3\text{O}_{7-\delta}$  was subtracted from the raw data. The resulting curves, which would then describe the change in magnetic susceptibility due to the substitution of Pr, could also be described with Eq. (1). The effective moment  $\mu_{\text{eff}}$  per Pr ion extracted from the fitting parameter  $C$  has an average value of  $2.87 \mu_B$ , which is smaller than the effective free ion moment for  $\text{Pr}^{3+}$  of  $3.58 \mu_B$ . We analyze the susceptibility data by writing the temperature-independent susceptibility as

$$\chi_0 = \chi^{\text{core}} + \chi^{\text{Pauli}} + \chi^{\text{Landau}}, \quad (2)$$

where  $\chi^{\text{core}}$  is the core diamagnetism term,  $\chi^{\text{Pauli}}$  is the Pauli paramagnetism due to the conduction electrons, and  $\chi^{\text{Landau}}$  is the diamagnetic orbital contribution due to the conduction electrons. The core diamagnetism may be estimated from tabulated values<sup>23</sup> [ $\text{Y}^{3+}$ : 12;  $\text{Pr}^{3+}$ : 20;  $\text{Ba}^{2+}$ : 32;  $\text{Cu}^{2+}$ : 11;  $\text{O}^{2-}$ : 12 (all in units of  $10^{-6}$  emu/mol)]. Representing the conduction-electron band effects by an effective mass,  $m^*$ , permits one to relate  $\chi^{\text{Pauli}}$  to  $\chi^{\text{Landau}}$  (Ref. 24):

$$\chi^{\text{Landau}} = -\frac{1}{3} \left( \frac{m}{m^*} \right)^2 \chi^{\text{Pauli}}. \quad (3)$$

By neglecting various enhancements, we approximate the effective mass  $m^*$  by the free electron mass  $m$ , so that  $\chi^{\text{Landau}} = -\frac{1}{3} \chi^{\text{Pauli}}$ . Then Eq. (2) is reduced to

$$\chi^{\text{Pauli}} = \frac{3}{2} (\chi_0 - \chi^{\text{core}}); \quad (4)$$

we estimated  $\chi^{\text{Pauli}}$  using these approximations. The values of  $\chi_0$ ,  $\chi^{\text{core}}$ , and  $\chi^{\text{Pauli}}$  are listed in Table II for  $\text{Y}_{1-x}\text{Pr}_x\text{Ba}_2\text{Cu}_3\text{O}_{7-\delta}$  ( $0 \leq x \leq 1.0$ ) along with values of the Curie-Weiss temperature  $\Theta$  and coefficient  $C$ .

We estimate the value of the electronic specific coefficient,  $\gamma$ , from the Pauli susceptibility using the free-electron conversion  $\gamma = \frac{1}{3} (\pi \kappa_B / \mu_B)^2 \chi^{\text{Pauli}}$ . This estimate does not take into account various enhancements to the susceptibility or specific heat which do not apply to each equally. This formula is only a very rough approximation; however, it is still important to get estimates of these critical parameters.

The desired  $\gamma$  values are used to compute the density of states at Fermi energy by the following formula:<sup>25</sup>

$$N(0) = (2\pi^2 \kappa_B^2 / 3)^{-1} \gamma = 7.97 \times 10^{30} \gamma, \quad (5)$$

where  $N(0)$  is in states/cm<sup>3</sup> erg spin direction and  $\gamma$  is in erg/cm<sup>3</sup> K<sup>2</sup> units. The values of  $\gamma$  and  $N(0)$  determined thus from the measured Pauli susceptibility are listed in Table III along with other parameters which are derived in the following.

The upper-critical-field  $H_{c2}$  was defined as the field where the magnetization  $M$  reaches the paramagnetic value at the corresponding temperature. In our experiments, the upper-critical-field  $H_{c2}$  was measured magnetically up to 50 kOe with the SQUID magnetometer for the superconducting  $\text{Y}_{1-x}\text{Pr}_x\text{Ba}_2\text{Cu}_3\text{O}_{7-\delta}$  ( $x = 0, 0.1, 0.2, 0.3, 0.35, 0.4, \text{ and } 0.45$ ).  $H_{c2}$  was taken as the value where the measured magnetization deviates from the high-field straight lines, within the experimental uncertainty in magnetization values. The self-consistency of this procedure may be ascertained by plotting the tem-

TABLE II. Susceptibility data for  $\text{Y}_{1-x}\text{Pr}_x\text{Ba}_2\text{Cu}_3\text{O}_{7-\delta}$ .

$x$	$\chi_0$ ( $10^{-7}$ emu/g)	$\Theta$ (K)	$C$ ( $10^{-4}$ emu/g)	$\chi^{\text{core}}$ ( $10^{-7}$ emu/g)	$\chi^{\text{Pauli}}$ ( $10^{-7}$ emu/g)
0.0	4.8	10.0	1.29	-2.90	11.6
0.1	6.0	0.2	3.20	-2.89	13.4
0.2	6.6	-5.2	3.75	-2.87	14.2
0.3	6.9	-11.7	5.92	-2.86	14.7
0.35	6.4	-4.2	6.30	-2.85	13.9
0.4	7.5	-8.4	6.68	-2.85	15.6
0.45	7.2	-6.0	8.29	-2.84	15.1
0.5	7.8	-8.5	8.10	-2.85	16.0
0.6	9.3	-4.4	8.20	-2.82	18.2
0.7	10.6	-5.2	10.40	-2.82	20.1
0.9	12.0	-4.6	11.90	-2.79	22.3
1.0	15.1	-7.3	15.30	-2.78	26.7

TABLE III. Superconducting and normal-state parameters for  $Y_{1-x}Pr_xBa_2Cu_3O_{7-\delta}$ .

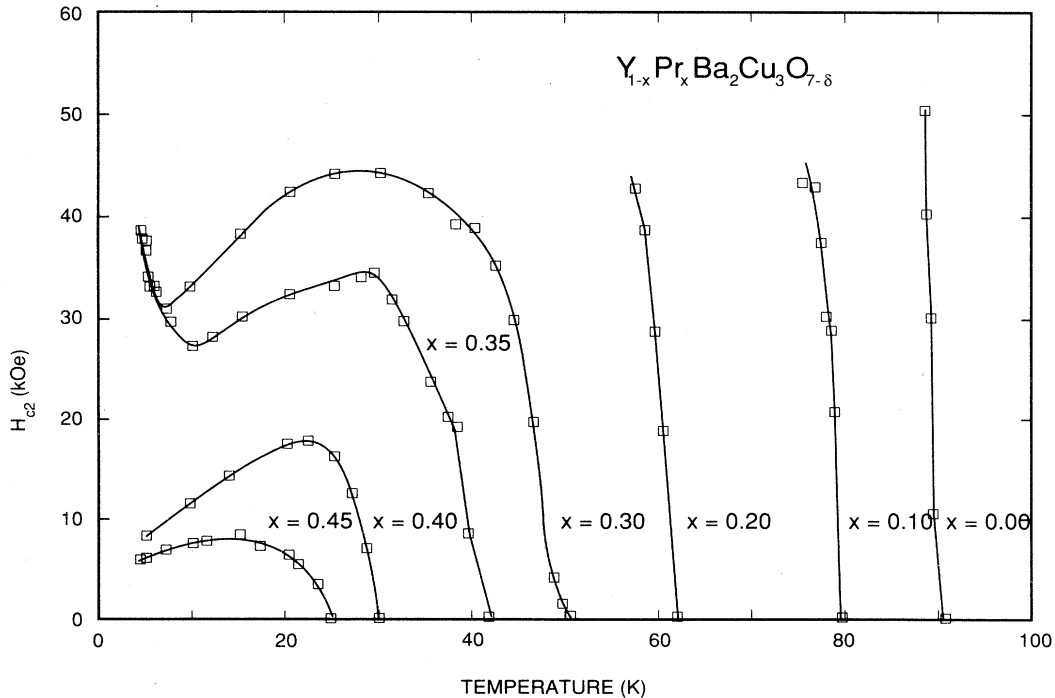
$x$	0	0.1	0.2	0.3	0.35	0.4	0.45	0.5	0.6	0.7	0.9	1.0
$T_c$ (K)	88.5	81.0	62.7	47.5	44.5	32	29.2					
$\Delta T_c$ (K)	2.0	9.8	8.3	9.2	10.8	7.0	9.6					
$-\left[\frac{dH_{c2}}{dT}\right]_{T=T_c}$ $\left(\frac{\text{kOe}}{\text{K}}\right)$	27.3	16.0	11.6	6.9	6.0	4.1	2.2					
$\alpha$	1.440	0.844	0.612	0.364	0.317	0.216	0.116					
$\gamma$ ( $\text{mJ}/\text{K}^2\text{cm}^3$ )	0.541	0.627	0.669	0.697	0.661	0.742	0.720	0.764	0.876	0.970	1.088	1.310
$\rho$ ( $\mu\Omega\text{cm}$ )	113.3	57.3	38.9	22.2	20.4	12.4	6.9					
$\xi_{GL}(0)$ ( $\text{\AA}$ )	12	16	21	32	35	50	71					
$\lambda_{GL}(0)$ ( $\text{\AA}$ )	726	540	506	439	435	400	312					
$\kappa_{GL}$	63	34	24	14	12	8	4					
$N(0)$ (states/eV atom spin)	0.915	1.065	1.041	1.188	1.126	1.268	1.234	1.312	1.504	1.673	1.884	2.271

perature dependence of the magnetic susceptibility measured at constant field. In our polycrystalline experiments we observe no evidence of flux lattice melting as reported in some single-crystal studies.<sup>26</sup>

The temperature dependence of  $H_{c2}$  is shown in Fig. 7. For all samples with  $x \geq 0.3$ ,  $H_{c2}(T)$  is smoothly bell shaped. Samples of  $x = 0.3$  and 0.35 have the indication of a low-temperature anomaly in the  $H_{c2}(T)$  data. The initial slope  $(-dH_{c2}/dT)_{T=T_c}$  decreases rapidly with increasing  $x$ .

The slope of the upper critical field near  $T_c$ , in con-

junction with the electronic heat-capacity coefficient estimated from the measured Pauli susceptibility, provides an estimate of certain normal-state and superconducting parameters. Values of the Ginzburg-Landau (GL) parameters<sup>27</sup> are derived using the BCS Gor'kov equations<sup>28</sup> near  $T_c$  in the dirty limit. The GL parameters  $\xi_{GL}$ ,  $\lambda_{GL}$ , and  $\kappa_{GL}$  depend only on quantities such as  $T_c$ ,  $\gamma$ , and the residual resistivity  $\rho$ . These calculated residual resistivity values are considerably lower than the values obtained experimentally at 100 K (see Fig. 4). This is to be expected since the GL calculations yield theoretical values for

FIG. 7.  $H_{c2}$  as a function of temperature for  $x = 0.0, 0.1, 0.2, 0.3, 0.35, 0.4,$  and  $0.45$ .

the resistance of an ideal (single-crystal) specimen at the lowest temperatures, in contrast to our power samples with grain boundary resistance and experimental porosity. Because of these differences, we limit our comparison to similar materials across the compositional range. This approach is still valid and provides useful information as noted in the forthcoming discussion section. The intrinsically short coherence length of the superconducting oxides ( $\sim 20$  Å) is not unlike the small coherence length ( $\sim 100$  Å) of many traditional superconductors in the dirty limit. Therefore, while direct applicability of the GL equations to the high- $T_c$  materials has not been substantiated, the short coherence length makes the approach reasonable. We note that the GL parameters derived in this manner are consistent with experimental results.

In Table III we present the values of the experimentally determined quantities, as well as the parameters derived from them. The values of  $T_c$  were determined from the midpoint of the resistivity drop. The values of  $(dH_{c2}/dT)_{T=T_c}$  are taken from Fig. 7, along with the Maki parameters<sup>29</sup>

$$\alpha = 5.2758 \times 10^{-2} \left[ \frac{dH_{c2}(\text{kOe})}{dT} \right]_{T=T_c}.$$

The residual resistivity  $\rho$  is determined from

$$\rho = 42.56\alpha/\gamma, \quad (6)$$

in units of  $\mu\Omega$  cm. The values of the GL parameters are then determined from the following equations:<sup>28</sup>

$$\xi_{\text{GL}}(T) = [8.57 \times 10^2 / (\rho T_c \gamma)^{1/2}] \left[ 1 - \frac{T}{T_c} \right]^{-1/2}, \quad (7)$$

$$\lambda_{\text{GL}}(T) = [6.42 \times 10^2 (\rho/T_c)^{1/2}] \left[ 1 - \frac{T}{T_c} \right]^{-1/2} \quad (8)$$

in units of Å, and

$$\kappa = 0.749[\gamma]^{1/2}\rho, \quad (9)$$

where all lengths are in units of Å, and  $\gamma$  is in units of  $\text{mJ}/\text{K}^2\text{cm}^3$ . The estimated value of  $\xi_{\text{GL}}$  increases rapidly with Pr content, while the corresponding value of  $\lambda_{\text{GL}}$  decreases with Pr content. The value of  $\kappa$  decreases with increasing Pr concentration. The  $\kappa$  values show that the  $\text{Y}_{1-x}\text{Pr}_x\text{Ba}_2\text{Cu}_3\text{O}_{7-\delta}$  ( $0 \leq x \leq 0.45$ ) compounds are extreme type-II superconductors. Based on the Maki parameter derived from the critical field slope at  $T_c$ , the derived value of the residual resistivity also decreases with increasing Pr content. This identification of the zero-pair-breaking Maki parameter with the critical-field slope may underestimate the residual resistivity for large Pr concentrations, since for larger pair breaking one expects the slope,  $(-dH_{c2}/dT)_{T_c}$ , to decrease due to the internal field generated by these interacting ions. Any correction of this nature would be small, perhaps causing the residual resistivity to saturate at some minimum value as the Pr concentration is increased. A correction of this type does not affect the analysis and conclusions in the following section.

## DISCUSSION

The primary challenge in the  $\text{Y}_{1-x}\text{Pr}_x\text{Ba}_2\text{Cu}_3\text{O}_{7-\delta}$  system is to explain the quenching of superconductivity due to Pr substitution. One possibility which was suggested early on is that the Pr ion exists as  $\text{Pr}^{4+}$ , which would imply that the extra electron (as opposed to  $\text{Pr}^{3+}$ ) cancels hole carriers in the Cu—O plane. As the carrier concentration is reduced, superconductivity is destroyed in a manner analogous to what happens as oxygen is removed from the parent  $\text{YBa}_2\text{Cu}_3\text{O}_{7-\delta}$  compound.<sup>30</sup>

A mixed valence state between  $\text{Pr}^{3+}$  and  $\text{Pr}^{4+}$  has in fact been proposed by several research groups on the basis of magnetic-susceptibility data.<sup>10-13,31,32</sup> The magnetic moment of the Pr ion is found to be intermediate between the free ion values for  $\text{Pr}^{3+}$  and  $\text{Pr}^{4+}$ . This has been interpreted to imply the presence of some fraction of  $\text{Pr}^{4+}$ . While our own susceptibility results agree with the previous values of the measured moment,<sup>10-13,31,32</sup> we disagree strongly that this is the only interpretation of these data. It is important to note that a reduced value of the Pr moment derived from susceptibility data can arise from crystal-field effects. This has been observed, for example, in the  $\text{RRh}_4\text{B}_4$  ( $R$ =rare earth) systems.<sup>33</sup> Without a detailed knowledge of the crystal-field levels, the magnetic moment by itself does not provide independent evidence for a  $\text{Pr}^{4+}$  valence.

In addition to the argument that there is no direct evidence for the presence of  $\text{Pr}^{4+}$ , there are a number of measurements which indicate that Pr is in the  $\text{Pr}^{3+}$  state across the entire compositional range. These include several x-ray-absorption measurements<sup>18,19</sup> and a photoemission study.<sup>34</sup> It has also been argued<sup>35</sup> from the variation of lattice parameters and Raman frequencies that the Pr is in the  $3+$  state. While the question of whether a small fraction of  $\text{Pr}^{4+}$  is present is still open, the majority of the data points towards the need for a different explanation for the destructive effect of Pr on superconductivity in this system.

In conventional superconductors, the presence of magnetic ions is usually incompatible with the superconducting state. In some cases such as the  $\text{RRh}_4\text{B}_4$  and  $\text{RMO}_6\text{S}_8$  materials,<sup>36</sup> superconductivity was found to exist where the magnetic ions were incorporated as full members of the unit cell. The  $\text{RBa}_2\text{Cu}_3\text{O}_7$  system can be termed the ultimate in magnetic superconductors, as the presence of the rare-earth ions does little or nothing to depress the superconductivity. This is believed to be due to the complete isolation of the electrons in the Cu—O planes from the magnetic ions.<sup>2-5</sup> The only exception for which the phase can be formed is Pr. One can then ask the question of whether the quenching of superconductivity by Pr is due to the more traditional magnetic pair-breaking interactions. While it is not clear why only Pr would be able to interact magnetically with the superconducting electrons, there is some evidence from photoemission work<sup>34</sup> that the Pr wave functions are hybridizing to a greater extent with the valence electrons than is true for the other rare-earth elements. This in fact makes good sense as the Pr  $4f$  wave functions are expected to be more extended spatially, due to its location at the far left of the

lanthanide series. In the following paragraphs we present arguments that magnetic pair breaking is occurring in this system. These considerations must be taken into account by any complete explanation of this system.

The first piece of evidence comes from the form of the  $T_c$  versus concentration curve, which was shown in Fig. 5. The depression of  $T_c$  upon the introduction of magnetic impurities is described well by the Abrikosov and Gor'kov (AG) theory.<sup>37</sup> In this theory it is assumed that a paramagnetic impurity spin  $\mathbf{S}$  interacts with the conduction electron spin density  $\mathbf{s}$  at the impurity site through an exchange interaction of the form

$$\mathcal{H}_{\text{int}} = \mathbf{J}\mathbf{S} \cdot \mathbf{s}, \quad (10)$$

where the exchange interaction parameter is denoted by  $J$ . It is this exchange interaction that lifts the degeneracy of the two states forming a Cooper pair. Such an interaction is, therefore, referred to as pair breaking. In general, the rare-earth impurities have unquenched orbital angular momentum. The appropriate states for calculating thermal averages are those of the total angular momentum  $\mathbf{J} = \mathbf{L} + \mathbf{S}$ . The exchange interaction, which always involves the spin, then becomes<sup>37</sup>

$$\mathcal{H} = \sum_i (g_J - 1) \mathcal{J} \mathbf{J}_i \cdot \mathbf{S}, \quad (11)$$

where  $\mathcal{J}$  is now the exchange parameter and  $g_J$  is the Landé  $g$  factor. Following tradition, we define

$$\Gamma = 2\pi n_i N(0) \mathcal{J}^2 (g_J - 1)^2 J(J+1)/4,$$

which characterizes the pair-breaking strength. Here  $n_i$  is the number density of impurities,  $N(0)$  is the density of electronic states at the Fermi energy, and  $(g_J - 1)^2 J(J+1)$  is the de Gennes factor. The theory predicts a rapid decrease of the transition temperature by the universal relation

$$\ln(T_c/T_c^P) = \psi(\frac{1}{2}) - \psi(\frac{1}{2} + \rho), \quad (12)$$

where  $\rho = \Gamma/\pi k_B T_c$ ,  $T_c^P$  is the  $T_c$  for "pure" material, and  $\psi$  is the digamma function. The solution of this equation can be obtained by a self-consistent method. The solid curve in Fig. 5 is a fit of  $T_c$  versus  $x$  using Eq. (12). All the experimental data fall onto this curve within the experimental error. Therefore, the Abrikosov and Gor'kov (AG) theory successfully fits the basic features of the experiment. While the  $T_c$ 's reported here differ slightly from Jee *et al.*,<sup>12</sup> both sets of data can be fit with an AG model. It is therefore reasonable to attribute the depression of  $T_c$  upon the introduction of magnetic Pr ions into  $\text{YBa}_2\text{Cu}_3\text{O}_{7-\delta}$  compounds to the pair-breaking mechanism. Using the values of  $J=4$ ,  $g_J = \frac{4}{5}$  for the  $\text{Pr}^{3+}$  Hund's rule ground state, one obtains a value for the coupling constant  $N(0)\mathcal{J}^2$  of  $7.08 \times 10^{-4}$  eV atom states/spin direction. We note that this value is roughly equal to the coupling constant between conduction electrons and magnetic  $\text{Tm}^{3+}$  moments in the system  $(\text{Tm}_x\text{Lu}_{1-x})\text{RuB}_2$ .<sup>38</sup> The consistency of these results suggests a similar magnetic pair-breaking mechanism which plays a role in depressing  $T_c$  in these different materials.

We estimate the value of the exchange interaction parameter between conduction electrons and magnetic Pr ions using the density of states  $N(0)$  of the host compound  $\text{YBa}_2\text{Cu}_3\text{O}_{7-\delta}$  determined earlier from the Pauli susceptibility along with the value of  $N(0)\mathcal{J}^2$  estimated from the Abrikosov-Gor'kov formula in the following discussion. We found a relatively low value on the order of  $\approx 0.028$  eV. This is in reasonable agreement with the values 0.02 eV in the rare-earth magnetic Chevrel phases.<sup>39</sup>

The second set of evidence comes from the behavior of the Pauli susceptibility with Pr concentration. As shown in Fig. 6 the Pauli susceptibility increases with the addition of Pr which agrees with the trend reported by Matsuda *et al.*<sup>11</sup> This is in sharp contrast to the behavior of this quantity when oxygen is removed from the parent  $\text{YBa}_2\text{Cu}_3\text{O}_{7-\delta}$  compound.<sup>40</sup> In that case it is found that the Pauli susceptibility decreases as the oxygen content is lowered. This is quite reasonable as the Pauli susceptibility is proportional to the density of states at the Fermi level. It has been shown that as oxygen is removed, the number of holes in the Cu—O plane is reduced.<sup>30,41</sup> The difference in behavior between the two methods of quenching superconductivity would imply that the effect of the Pr cannot be just to remove holes from the plane, in analogy to the  $\text{YBa}_2\text{Cu}_3\text{O}_{7-\delta}$  oxygen depleted case. It can be speculated that the increase in the Pauli susceptibility with Pr content may be related to magnetic effects, i.e., Stoner enhancement factors.<sup>42,43</sup> To separate conclusively the density-of-states effects from magnetic effects would require a knowledge of the Sommerfeld constant gamma, which has not yet been determined for the  $\text{Y}_{1-x}\text{Pr}_x\text{Ba}_2\text{Cu}_3\text{O}_{7-\delta}$  system. It should also be noted that as oxygen is removed from  $\text{YBa}_2\text{Cu}_3\text{O}_{7-\delta}$ , a phase change occurs, from orthorhombic to tetragonal symmetry. Here no phase change occurs near the  $x=0.5$  critical concentration.

The third set of evidence is completely new, and comes from our results for the behavior of the upper critical fields (Fig. 7). In conventional superconductors, the critical fields increase monotonically with decreasing temperature. It is well established,<sup>36</sup> however, that in certain cases the presence of magnetic pair-breaking interactions can cause the critical-field curves to have a maximum as a function of  $T$ . This occurs as the internal fields generated by the magnetic ions increase dramatically at the lower temperatures. This "bell shape" of the critical fields can occur even if the interactions are antiferromagnetic in type.<sup>36</sup> In the most extreme cases, the material can reenter the normal state, as is the case for  $\text{ErRh}_4\text{B}_4$  and  $\text{HoMo}_6\text{S}_8$ .<sup>36</sup> The critical-field curves shown in Fig. 7 exhibit this bell-shaped behavior for  $x \geq 0.3$ , indicating the importance of magnetic interactions in this system.

If one adopts the point of view that magnetic pair breaking is quenching the superconductivity, one puzzling observation is the change in resistivity behavior with Pr concentration. Upturns in resistivity are seen in Fig. 3 even for superconducting samples ( $0.35 < x < 0.45$ ). In the absence of a proper model for the normal-state resistivity as a function of temperature, it is particularly instructive to consider a plot of the resistivity at a specific

temperature in the normal state of all the materials. The plot of  $\rho(100\text{ K})$  versus  $x$  in Fig. 4 shows a sharp increase in resistivity after the destruction of superconductivity. The value of the resistivity stays near the value of  $10\text{ m}\Omega\text{ cm}$  through  $x=0.6$ , followed by an increase to near  $100\text{ }\Omega\text{ cm}$  for  $x=1.0$ . This change of nearly 4 orders of magnitude, taking place at concentrations where the superconductivity is already quenched, may indicate the presence of more than one mechanism for conductivity in the normal state. The upturn in the resistivity is often cited as compelling evidence for the metal-insulator transition.<sup>8,12,15</sup> We feel that the resistivity in these materials is poorly understood, and that there is in fact no direct evidence for a depletion of charge carriers in the Cu—O plane over the range  $0 < x < 0.5$ .

The following is a summary of the properties of the Pr-doped system which we feel must be explained by any complete theoretical model.

1. The resistivity shows a negative slope even before the superconductivity is destroyed for  $x < 0.5$ .
2. The resistivity at 100 K versus  $x$  shows a sharp increase for  $x < 0.7$ .
3. The system remains orthorhombic over the range where superconductivity is quenched.
4. Raman spectroscopy shows that no abrupt change in the phonon spectra occurs at the critical concentration ( $x=0.5$ ).
5. Several types of spectroscopies and correlations in-

dicate that Pr exists in the  $3+$  state in this system.

6. The depression of  $T_c$  with Pr follows an AG model.
7. The Pauli susceptibility increases with Pr content.
8. The critical fields show a bell-shaped behavior for  $x \geq 0.30$ .

#### SUMMARY

We have determined a procedure for making single-phase samples with well-determined oxygen contents, as characterized by x-ray diffraction, magnetization, resistivity, TGA, DTA, and Raman spectroscopy. The critical fields were determined from magnetization data, and in conjunction with the Pauli susceptibility were used to derive superconducting and normal-state parameters. The  $H_{c2}$  curves were found to show bell-shaped behavior for  $x \geq 0.3$ . Along with the increase in the Pauli susceptibility and the good fit of the  $T_c$  versus  $x$  data to the AG model, it is argued that magnetic pair-breaking interactions play a significant role in quenching the superconductivity, and must be included in any theoretical model for this system.

#### ACKNOWLEDGMENTS

Research at Davis and Livermore was performed under the auspices of the U.S. Department of Energy for Lawrence Livermore National Laboratory under Contract No. W-7405-ENG-48.

- <sup>1</sup>M. K. Wu, J. R. Ashburn, C. J. Torng, P. H. Hor, R. L. Meng, L. Gao, Z. J. Huang, Y. Q. Wang, and C. W. Chu, *Phys. Rev. Lett.* **58**, 908 (1987).
- <sup>2</sup>K. N. Yang, Y. Dalichaouch, J. M. Ferreria, B. W. Lee, J. J. Neumeir, M. S. Torikachvili, H. Zhou, M. B. Maple, and R. R. Hake, *Solid State Commun.* **63**, 515 (1987).
- <sup>3</sup>Z. Fisk, J. D. Thompson, E. Zirngiebl, J. L. Smith, and S. W. Cheong, *Solid State Commun.* **62**, 743 (1987).
- <sup>4</sup>P. H. Hor, R. L. Meng, Y. Q. Wang, L. Gao, Z. J. Huang, J. Bechtold, K. Forster, and C. W. Chu, *Phys. Rev. Lett.* **58**, 1891 (1987).
- <sup>5</sup>D. W. Murphy, S. Sunshine, R. B. Van Dover, R. J. Cava, B. Batlogg, S. M. Zahurak, and L. F. Schneemeyer, *Phys. Rev. Lett.* **58**, 1888 (1987).
- <sup>6</sup>K. N. Yang, B. W. Lee, M. B. Maple, and S. S. Laderman, *Appl. Phys. A* **46**, 229 (1988).
- <sup>7</sup>L. Soderholm, K. Zhang, D. G. Hinks, M. A. Beno, J. D. Jorgenson, C. U. Segre, and I. K. Schuller, *Nature* **328**, 604 (1987).
- <sup>8</sup>Y. Dalichaouch, M. S. Torikachvili, E. A. Early, B. W. Lee, C. L. Seaman, K. N. Yang, H. Zou, and M. B. Maple, *Solid State Commun.* **65**, 1001 (1987).
- <sup>9</sup>K. K. Liang, X. T. Xu, S. S. Xie, G. H. Rao, X. Y. Shao, and Z. G. Duan, *Z. Phys. B* **69**, 137 (1987).
- <sup>10</sup>Y. Dalichaouch, M. S. Torikachvili, E. A. Early, B. W. Lee, C. L. Seaman, K. N. Yang, H. Zou, and M. B. Maple, *Solid State Commun.* **65**, 1001 (1987).
- <sup>11</sup>A. Matsuda, K. Kinoshita, T. Ishii, H. Shibata, T. Wantabe, and T. Yamada, *Phys. Rev. B* **38**, 2910 (1988).
- <sup>12</sup>C. S. Jee, A. Kebebe, D. Nichols, J. E. Crow, I. Mihalisin, G. H. Meyer, I. Perez, R. E. Salomon, and P. Schlottmann, *Solid State Commun.* **69**, 379 (1989).
- <sup>13</sup>C. S. Jee, A. Kebebe, T. Yuen, S. H. Bloom, M. V. Kuric, J. E. Crow, R. P. Guertin, T. Mihalisin, G. H. Myer, and P. Schlottmann (unpublished).
- <sup>14</sup>N. Sankar, V. Sankaranarayanan, L. S. Vaidyanathan, G. Rangarajan, R. Srinivasan, K. A. Thomas, U. V. Varadaraju, and G. V. Subba Rao, *Solid State Commun.* **67**, 391 (1988).
- <sup>15</sup>A. P. Goncalves, I. C. Santos, E. B. Lopes, R. T. Henriques, and M. Almeida, *Phys. Rev. B* **37**, 7476 (1988).
- <sup>16</sup>B. Renker, F. Gompf, E. Gering, G. Roth, W. Reichardt, D. Ewert, H. Rietschel, and H. Mutka, *Z. Phys. B* **71**, 437 (1988).
- <sup>17</sup>J. J. Neumeier, M. B. Maple, and M. S. Torikachvili, *Physica C* **156**, 574 (1988).
- <sup>18</sup>U. Neukirch, C. T. Simmons, P. Sladeczek, C. Laubschat, O. Strebel, G. Kaindl, and D. D. Sarma, *Europhys. Lett.* **5**(6), 567 (1988).
- <sup>19</sup>F. W. Lytle, R. B. Gregor, E. M. Larson, and J. Wong (unpublished).
- <sup>20</sup>R. Bhadra, T. O. Brun, M. A. Beno, B. Dabrowski, D. G. Hinks, J. Z. Liu, J. D. Jorgenson, L. J. Nowici, A. P. Paulikas, I. K. Schuller, C. U. Segre, L. Soderholm, B. Veal, H. H. Wang, J. M. Williams, K. Zhang, and M. Grimsditch, *Phys. Rev. B* **37**, (1988).
- <sup>21</sup>H. B. Radousky, J. L. Peng, R. N. Shelton, and K. F. McCarthy, *Phys. Rev. B* **39**, 12383 (1989).
- <sup>22</sup>S. W. Hsu, M. F. Tai, C. C. Chen, H. C. Ku, H. D. Yang, and R. N. Shelton, *Chin. J. Phys.* **26**, S113 (1988).
- <sup>23</sup>P. W. Selwood, *Magnetochemistry*, 2nd ed. (Interscience, New York, 1970), p. 78.
- <sup>24</sup>R. M. White, *Quantum Theory of Magnetism* (McGraw-Hill, New York, 1970), p. 86.
- <sup>25</sup>T. P. Orlando, E. J. McNiff, Jr., S. Foner, and M. R. Beasley, *Phys. Rev. B* **19**, 4545 (1979).

- <sup>26</sup>P. L. Gammel, L. F. Schneemeyer, J. V. Waszczak, and D. J. Bishop, *Phys. Rev. Lett.* **61**, 1666 (1988).
- <sup>27</sup>B. Serin, in *Superconductivity*, edited by R. D. Parks (Decker, New York, 1968), p. 925.
- <sup>28</sup>N. R. Werthamer, in *Superconductivity*, edited by R. D. Parks (Decker, New York, 1968), p. 321.
- <sup>29</sup>N. R. Werthamer, E. Helfand, and P. C. Hohenberg, *Phys. Rev.* **147**, 295 (1966).
- <sup>30</sup>R. J. Cava, B. Batlogg, C. H. Chen, E. A. Rietman, S. A. Zahurak, and D. Werder, *Nature* **329**, 423 (1987).
- <sup>31</sup>E. Moran, U. Amador, M. Barahona, M. A. Alario-Franco, A. Vegas, and J. Rodriguez-Carvajal, *Solid State Commun.* **67**, 369 (1988).
- <sup>32</sup>C. Thomsen, R. Liu, M. Cardona, U. Amador, and E. Moran, *Solid State Commun.* **67**, 271 (1988).
- <sup>33</sup>B. D. Dunlap and D. G. Niarchos, *Solid State Commun.* **44**, 1577 (1982).
- <sup>34</sup>J.-S. Kaus, J. W. Allen, Z.-X. Shen, W. P. Ellis, J. J. Yeh, B.-W. Lee, M. B. Maple, W. E. Spicer, and I. Lindau, *J. Less-Common Met.* 148-149 (1989).
- <sup>35</sup>H. J. Rosen, R. M. McFarlane, E. M. Engler, V. Y. Lee, and R. D. Jacowitz, *Phys. Rev. B* **38**, 2460 (1988).
- <sup>36</sup>See, for example, *Superconductivity in Ternary Compound II*, Vol. 34 of *Topics in Current Physics*, edited by M. B. Maple and O. Fischer (Springer-Verlag, Berlin, 1982).
- <sup>37</sup>A. A. Abrikosov and L. P. Gor'kov, *Zh. Eksp. Teor. Fiz.* **39**, 1781 (1960) [*Sov. Phys.—JETP* **12**, 1243 (1961)].
- <sup>38</sup>H. C. Ku and R. N. Shelton, *Solid State Commun.* **40**, 237 (1981).
- <sup>39</sup>O. Fisher, *Appl. Phys.* **16**, 1 (1978).
- <sup>40</sup>T. Takabatake, M. Ishikawa, and T. Sugano, *Jpn. J. Appl. Phys.* **26**, 1859 (1987).
- <sup>41</sup>Y. Tokura, J. B. Torrance, T. C. Huang, and A. I. Nazzari, *Phys. Rev. B* **38**, 7156 (1988).
- <sup>42</sup>E. C. Stoner, *Proc. R. Soc. London, Ser. A* **165**, 372 (1938).
- <sup>43</sup>E. P. Wohlfarth, *Proc. R. Soc. London, Ser. A* **303**, 127 (1968).